Synchronized clusters in coupled map networks. II. Stability analysis

R. E. Amritkar,* Sarika Jalan,† and Chin-Kun Hu‡
[1]*Physical Research Laboratory, Navrangpura, Ahmedabad 380 009, India*
[2]*Institute of Physics, Academia Sinica, Nankang, Taipei 11529, Taiwan*
(Received 16 June 2004; published 19 July 2005)

We study self-organized and driven synchronization in some simple coupled map networks, namely globally coupled networks and complete bipartite networks, using both linear stability analysis and Lyapunov function approach and determine stability conditions for synchronization. The phase diagrams for the networks studied here have features very similar to the different kinds of structurally similar networks studied in Part I. Lyapunov function approach shows that when any two nodes are in driven synchronization, all the coupling terms in the difference between the variables of these two nodes cancel out, whereas when they are in self-organized synchronization, the direct coupling term between the two nodes adds an extra term while the other couplings cancel out. We also discuss the conditions for the occurrence of a floating node and suggest that the fluctuations of the conditional Lyapunov exponent about zero can be a criterion for its occurrence.

DOI: 10.1103/PhysRevE.72.016212 PACS number(s): 05.45.Ra, 05.45.Xt, 89.75.Fb, 89.75.Hc

I. INTRODUCTION

In Part I [1] of this paper we presented results of the numerical study of synchronization and cluster formation in coupled maps on different networks. Starting from random initial conditions the asymptotic behavior of these coupled map networks (CMNs) has revealed two interesting phenomena. First, there are two different mechanisms leading to two types of synchronized clusters. There are clusters with dominant intracluster couplings which are referred as *self-organized* clusters and there are clusters with dominant intercluster coupling which are referred as *driven* clusters [1,2]. The numerical studies reveal several clusters of both types as well as clusters of the mixed type where both mechanisms contribute. Second, there are floating nodes which show intermittent behavior between synchronous behavior with some cluster and an independent evolution. The residence times of a floating node in a synchronized cluster show an exponential distribution.

In the present paper we study the stability of synchronized dynamics of some simple coupled map networks (CMN) with a view to get a better understanding of the two mechanisms of cluster formation discussed above. For this study we use both linear stability analysis [3–9] and Lyapunov function approach [10,11]. As an example of networks showing self-organized synchronized clusters we take globally coupled maps [12] and for driven synchronized clusters we take complete bipartite coupled maps [13]. The Lyapunov function approach indicates that the self-organized behavior has its origin in the decay term arising due to intracluster couplings in the difference between the variables of any two synchronized nodes while the driven behavior has its origin in the cancellation of the intercluster couplings.

Synchronization of two dynamical variables is indicated by the appearance of some relation between the functionals of two variables [14,15,1,2]. In this paper we will mostly concentrate on exact synchronization, where the values of the dynamical variables associated with nodes are equal. Though the numerical work in Part I was carried out using phase synchronization, it is not easy to treat phase synchronization analytically and hence for the analytical work we restrict ourselves to exact synchronization. Interestingly the phase diagrams obtained using exact synchronization for the simple networks studied here have considerable similarity with those obtained in Part I numerically for more complex networks. Thus analytic study of simple networks can help us in understanding the behavior of more complex networks.

The stability analysis for the simple networks allows us to draw some conclusions about the occurrence of the floating nodes. We suggest that the conditional Lyapunov exponents can be useful for this analysis and the general conclusions are in agreement with the numerical findings.

The present paper is organized as follows. In Sec. II we study the stability conditions of synchronized states of the globally coupled networks and complete bipartite networks. We also point out the similarity of these analytical results obtained for the simple networks with those observed numerically for complex networks in Part I and discuss possible reasons for this similarity. Section III discusses some aspects of the occurrence of the floating nodes. Section IV concludes the paper.

II. STABILITY ANALYSIS

We now present the stability analysis of synchronized states in globally coupled networks and complete bipartite networks. We consider stability of both chaotic and periodic states. We find that it is sufficient to treat fixed point and period two orbits to get a reasonable picture of the phase diagram.

A. Globally coupled networks

Globally coupled networks have all pairs of nodes connected to each other, i.e., $N_c=N(N-1)/2$ where N is the total

*Email address: amritkar@prl.ernet.in
†Email address: sarika@prl.ernet.in
‡Email address: huck@phys.sinica.edu.tw

number of nodes and N_c is the total number of connections. For such global coupling we write our dynamical model [Eq. (1) of Part I] as

$$x_{t+1}^i = (1-\epsilon) f(x_t^i) + \frac{\epsilon}{N-1} \sum_{j \neq i, j=1}^{N} g(x_t^j), \tag{1}$$

where x_t^i, $i=1,2,\ldots,N$ is the dynamical variable of the ith node at the tth time step, and ϵ is the coupling strength ($0 \leqslant \epsilon \leqslant 1$). The function $f(x)$ defines the local nonlinear map and the function $g(x)$ defines the nature of coupling between the nodes. Though most of the analysis is general, we illustrate the results using two types of the coupling functions as in Part I,

$$g(x) = x, \tag{2a}$$

$$g(x) = f(x). \tag{2b}$$

We refer to the first type of coupling as linear and the latter as nonlinear. Note that the nonlinear coupling corresponds to a diffusive type of coupling.

The state $x_t^1 = x_t^2 = \cdots = x_t^N = x_t$ is the complete or fully synchronized state of the globally coupled network. We now consider the stability of this state.

1. Linear stability analysis

The Jacobian matrix at time t for the complete synchronized state is

$$J_t = \begin{pmatrix} (1-\epsilon) f_t' & \frac{\epsilon}{N-1} g_t' & \cdots & \frac{\epsilon}{N-1} g_t' \\ \frac{\epsilon}{N-1} g_t' & (1-\epsilon) f_t' & \cdots & \frac{\epsilon}{N-1} g_t' \\ \vdots & \vdots & \vdots & \vdots \\ \frac{\epsilon}{N-1} g_t' & \frac{\epsilon}{N-1} g_t' & \cdots & (1-\epsilon) f_t' \end{pmatrix} \tag{3}$$

where f_t' and g_t' are the derivative at the synchronous value x_t. Eigenvectors of the above Jacobian matrix are

$$E_m = \left[\exp\left(2\pi i \frac{m}{N}\right), \exp\left(4\pi i \frac{m}{N}\right), \ldots, \exp\left(2N\pi i \frac{m}{N}\right) \right]^T, \tag{4}$$

where $m=0,1,\ldots,N-1$ and T denotes the transpose. The eigenvector E_0 defines the synchronization manifold while the remaining are the transverse eigenvectors. From these eigenvectors we find that J_t has an eigenvalue $(1-\epsilon) f_t' + \epsilon g_t'$ corresponding to the eigenvector E_0 and $(N-1)$-fold degenerate eigenvalues $(1-\epsilon) f_t' - \epsilon/N-1 g_t'$. Lyapunov exponents can be written in terms of the eigenvalues of Jacobian matrix as

$$\lambda_1 = \lim_{\tau \to \infty} \frac{1}{\tau} \sum_{t=1}^{\tau} \ln \left| (1-\epsilon) f_t' + \epsilon g_t' \right|, \tag{5a}$$

$$\lambda_2 = \lambda_3 \cdots = \lambda_N = \lim_{\tau \to \infty} \frac{1}{\tau} \sum_{t=1}^{\tau} \ln \left| (1-\epsilon) f_t' - \frac{\epsilon}{N-1} g_t' \right|. \tag{5b}$$

Lyapunov exponents $\lambda_2, \lambda_3, \ldots, \lambda_n$ are the transverse Lyapunov exponents and for the stability of the synchronous orbits all the transverse Lyapunov exponents should be negative.

Coupling function $g(x)=f(x)$. Globally coupled maps are studied extensively with the $g(x)=f(x)$ type of diffusive coupling and the linear stability analysis is done to decide the stability of complete synchronized solution [3–5]. Lyapunov exponents are given by

$$\lambda_1 = \lambda_u = \lim_{\tau \to \infty} \frac{1}{\tau} \sum_{t=1}^{\tau} \ln |f'(x_t)|, \tag{6a}$$

$$\lambda_2 = \lambda_3 = \cdots = \lambda_N = \lambda_u + \ln(1-\epsilon), \tag{6b}$$

where λ_u is the Lyapunov exponent of the uncoupled map. The critical value of the coupling strength ϵ_c beyond which the synchronized state with all nodes synchronized with each other is stable, is given by

$$\epsilon_c = 1 - e^{-\lambda_u}. \tag{7}$$

For $f(x)=\mu x(1-x)$ and $\mu=4$, $\lambda_u = \ln 2$, we get $\epsilon_c = 0.5$. This result is consistent with the numerical observation in Part I that for large coupling strengths we get a single self-organized cluster as the number of connections become of the order of N^2.

Coupling function $g(x)=x$. From the expressions (5a) and (5b), it is difficult to determine when the synchronous orbits are stable. Rather it is easier to determine the stability of the synchronous orbits using the Lyapunov function which we will consider in the next section. Here, we consider some special cases when coupled dynamics of the complete synchronized state lies on the periodic or fixed point attractors.

Case I. Synchronization to fixed point. First we consider the fixed point $X^* = f(X^*)$ of the complete synchronized state. Using Eqs. (5a) and (5b) and for $f' < 0$ which is the interesting case, the fixed point is easily found to be stable in the range

$$\frac{|f'| - 1}{|f'| - \frac{1}{N-1}} < \epsilon < 1. \tag{8}$$

For $N=2$ this solution is not stable and the range of stability increases with N. This is a surprising result since with increasing N the number of transverse eigenvectors along which the synchronized solution can become unstable also increases. This feature of increasing range of stability with N is more general and will be noticed for other solutions also as will be discussed in subsequent analysis. For large N the synchronous fixed point is stable for

$$\frac{|f'|-1}{|f'|} < \epsilon < 1. \tag{9}$$

For $f(x)$ given by the logistic map, $X^*=1-1/\mu$, the range of stability of the synchronous fixed point is given by

$$\frac{\mu-3}{\mu-2-\frac{1}{N-1}} < \epsilon < 1. \tag{10}$$

Case II. Synchronization to period two orbit. We now consider synchronous period two solution. Let X_1 and X_2 be the values of the synchronized variables at consecutive time steps. The Lyapunov exponents can be obtained using Eqs. (5a) and (5b). The conditions for the stability of the period two solution are

$$\ln|[(1-\epsilon)f_1'+\epsilon][(1-\epsilon)f_2'+\epsilon]| < 0, \tag{11a}$$

$$\ln\left|\left((1-\epsilon)f_1'-\frac{\epsilon}{N-1}\right)\left((1-\epsilon)f_2'-\frac{\epsilon}{N-1}\right)\right| < 0, \tag{11b}$$

where f_1' and f_2' are the derivatives at X_1 and X_2, respectively.

For $f(x)$ given by the logistic map, the period two synchronized solution is given by

$$X_{1,2}=\frac{1+\epsilon+\mu(1-\epsilon)\pm\sqrt{\epsilon(\epsilon-2)(\mu-1)^2-3-2\mu+\mu^2}}{2\mu(1-\epsilon)}. \tag{12}$$

For $\mu=4$,

$$X_{1,2}=\frac{5-3e+\sqrt{5-18e+9e^2}}{8(1-e)}. \tag{13}$$

Thus the range of stability of the period two synchronized solution can be obtained exactly and for $\mu=4$ the range is

$$1-\frac{\sqrt{54}}{9} < \epsilon < \frac{10+\frac{1}{N-1}-\sqrt{60+\frac{30}{N-1}+\frac{6}{(N-1)^2}}}{8-\frac{2}{N-1}-\frac{1}{(N-1)^2}}. \tag{14}$$

For $N=2$, this gives the ϵ range of stability as (0.18…,0.24…) while for large N, this range of stability for ϵ values expands to (0.18…,0.28…) [16]. Note that this range of stability approximately corresponds to region II-S in Fig. 1 of Part I.

2. Lyapunov function analysis

We define Lyapunov function for any pair of nodes i and j as

$$V_t^{ij}=(x_t^i-x_t^j)^2. \tag{15}$$

Clearly, $V_{ij}(t)\geqslant 0$ and the equality holds only when the nodes i and j are exactly synchronized. For the asymptotic global stability of the synchronized state in a region, Lyapunov function should satisfy the following condition in that region:

$$V_{t+1} < V_t. \tag{16}$$

This condition can also be written as

$$\frac{V_{t+1}}{V_t} < 1. \tag{17}$$

For the globally coupled networks the Lyapunov function of Eq. (15) becomes

$$V_{t+1}^{i,j}=\left[(1-\epsilon)[f(x_t^i)-f(x_t^j)]-\frac{\epsilon}{N-1}[g(x_t^i)-g(x_t^j)]\right]^2. \tag{18}$$

Performing Taylor expansion around x_t^j, we get

$$\frac{V_{t+1}}{V_t}=\left[(1-\epsilon)f'(x_t^j)-\frac{\epsilon}{N-1}g'(x_t^j)+\frac{x_t^i-x_t^j}{2}\left((1-\epsilon)f''(x_t^j)-\frac{\epsilon}{N-1}g''(x_t^j)\right)+O((x_t^1-x_t^2)^2)\right]^2. \tag{19}$$

Coupling function $g(x)=f(x)$. In this case the expression (19) simplifies to

$$\frac{V_{t+1}}{V_t}=\left(1-\frac{N}{N-1}\epsilon\right)^2\left[f'(x_t^j)+\frac{x_t^i-x_t^j}{2}f''(x_t^j)+O((x_t^1-x_t^2)^2)\right]^2.$$

If the expression in the square bracket on the right-hand side is bounded then for large N there will be a critical value of ϵ beyond which the condition (17) will be satisfied and the globally synchronized state will be stable. For $f(x)=\mu x(1-x)$ and using $(0\leqslant x_t^i+x_t^j\leqslant 2)$, we get the following range of coupling strength values for which the globally synchronized state is stable.

$$\frac{N-1}{N}\left(1-\frac{1}{\mu}\right) < \epsilon \leqslant 1 < \frac{N-1}{N}\left(1+\frac{1}{\mu}\right). \tag{20}$$

For $\mu=4$ and for very large N, coupling strength range is $0.75<\epsilon<1$. A better ϵ range is obtained by putting more realistic bounds as $X^-\leqslant x_t^i+x_t^j\leqslant X^+$, which gives the range of stability as

$$\frac{N-1}{N}\left(1-\frac{1}{\mu A}\right) < \epsilon \leqslant 1, \tag{21}$$

where $A=\max(|1-X^+|,|1-X^-|)$.

Coupling function $g(x)=x$. In this case, for the logistic map, the expression (19) simplifies to

$$\frac{V_{t+1}^{ij}}{V_t}=\left[(1-\epsilon)[1-(x_t^i+x_t^j)]-\frac{\epsilon}{N-1}\right]^2. \tag{22}$$

Since $0\leqslant x_t^i+x_t^j\leqslant 2$ we get a range of ϵ values for which the globally synchronized state is stable [Eq. (17)]

TABLE I. Eigenvalues and eigenvectors of Jacobian matrix [Eq. (26)] for the bipartite synchronized state of the complete bipartite network.

Set	Eigenvectors	Eigenvalue	No. of eigenvalues	Condition
A	$(\alpha_1 \cdots \alpha_{N_1}, 0 \cdots 0)$	$(1-\epsilon)f_1'$	N_1-1	$\Sigma\alpha=0$
B	$(0 \cdots 0, \beta_1 \cdots \beta_{N_2})$	$(1-\epsilon)f_2'$	N_2-1	$\Sigma\beta=0$
C	$(\alpha, \cdots, \alpha, \beta, \cdots, \beta)$		2	

$$\frac{\mu-1}{\mu-\frac{1}{N-1}} < \epsilon < \frac{\mu+1}{\mu-\frac{1}{N-1}}, \tag{23}$$

which for large N reduces to

$$\frac{\mu-1}{\mu} < \epsilon < \frac{\mu+1}{\mu}. \tag{24}$$

For $\mu=4$, we get the coupling strength range $0.75 < \epsilon \leqslant 1$ for which the globally synchronized state is stable. We also note that for $N=2$ the condition (23) for synchronization is not satisfied for any value of $\epsilon \leqslant 1$.

These results are consistent with the numerical observation in Part I of a large self-organized cluster for large coupling strengths as the number of connections increases.

B. Complete bipartite networks

A complete bipartite network consists of two sets of nodes with each node of one set connected with all the nodes of the other set. Clearly this type of network is an ideal example for studying driven synchronization. We take a bipartite network consisting of two sets of nodes, $N=N_1+N_2$, with each node of N_1 connected to every node of N_2 and there are no connections between the nodes of the same set [13]. Our model [Eq. (1) of Part I] for the coupled complete bipartite network can be written as

$$x_{t+1}^i = (1-\epsilon)f(x_t^i) + \frac{\epsilon}{N_2}\sum_{j=N_1+1}^{N} g(x_t^j)$$

$$\text{for } i = 1, \ldots, N_1,$$

$$x_{t+1}^i = (1-\epsilon)f(x_t^i) + \frac{\epsilon}{N_1}\sum_{j=1}^{N_1} g(x_t^j)$$

$$\text{for } i = N_1+1, \ldots, N. \tag{25}$$

We define a bipartite synchronized state of the bipartite network as the one that has all N_1 elements of the first set synchronized to some value, say $X_1(t)$, and all N_2 elements of the second set synchronized to some other value, say $X_2(t)$.

1. Linear stability analysis

Linear stability analysis of the bipartite synchronized state can be done using the Jacobian matrix,

$$J_t = \begin{pmatrix} (1-\epsilon)f_1' & 0 & \ldots & 0 & \frac{\epsilon}{N_2}g_2' & \frac{\epsilon}{N_2}g_2' & \ldots & \frac{\epsilon}{N_2}g_2' \\ \vdots & \vdots & \vdots & \vdots & \vdots & \vdots & \vdots & \vdots \\ 0 & 0 & \ldots & (1-\epsilon)f_1' & \frac{\epsilon}{N_2}g_2' & \frac{\epsilon}{N_2}g_2' & \ldots & \frac{\epsilon}{N_2}g_2' \\ \frac{\epsilon}{N_1}g_1' & \frac{\epsilon}{N_1}g_1' & \ldots & \frac{\epsilon}{N_1}g_1' & (1-\epsilon)f_2' & 0 & \ldots & 0 \\ \vdots & \vdots & \vdots & \vdots & \vdots & \vdots & \vdots & \vdots \\ \frac{\epsilon}{N_1}g_1' & \frac{\epsilon}{N_1}g_1' & \ldots & \frac{\epsilon}{N_1}g_1' & 0 & 0 & \ldots & (1-\epsilon)f_2' \end{pmatrix}, \tag{26}$$

where f_1' (f_2') and g_1' (g_2') are the derivative of $f(x)$ and $g(x)$, respectively, at X_1 (X_2). It is easy to see that the eigenvectors and eigenvalues of the above Jacobian matrix can be divided into three sets, A, B, and C (see Table I).

Here, $(\alpha_1, \ldots, \alpha_{N1})$, $(\beta_1, \ldots, \beta_{N2})$, and α, β are complex numbers satisfying the conditions specified in the last column. The two eigenvalues corresponding to the set C are the eigenvalues of the matrix

$$\begin{pmatrix} (1-\epsilon)f_1' & \epsilon g_2' \\ \epsilon g_1' & (1-\epsilon)f_2' \end{pmatrix}. \tag{27}$$

We make the following observations. (a) The three sets of eigenvectors, A, B, and C, are orthogonal to each other and the total space of eigenvectors may be written as a sum of these three sets. (b) The three sets of eigenvectors do not mix with each other under time evolution. (c) The eigenvectors belonging to the first two sets (A and B) are also the eigenvectors of the product of any number of Jacobian matrices under time evolution. (d) The set of eigenvectors C defines the synchronization manifold. The other two sets of eigenvectors A and B are transverse to the synchronization manifold.

Lyapunov exponents corresponding to the transverse eigenvectors can be easily written as

$$\lambda_1 = \ln|(1-\epsilon)| + \lim_{\tau\to\infty} \frac{1}{\tau}\sum_{t=1}^{\tau} \ln|f'(X_1)|, \tag{28a}$$

$$\lambda_2 = \ln|(1-\epsilon)| + \lim_{\tau\to\infty} \frac{1}{\tau}\sum_{t=1}^{\tau} \ln|f'(X_2)|, \tag{28b}$$

and λ_1 and λ_2 are, respectively, N_1-1 and N_2-1 fold degenerate. The synchronized state is stable provided the transverse Lyapunov exponents are negative. If f' is bounded as is the case for the logistic map then from Eqs. (28) we see that for ϵ larger than some critical value, $\epsilon_b(<1)$, the bipartite synchronized state will be stable. Note that this bipartite synchronized state will be stable even if one or both of the remaining Lyapunov exponents corresponding to the set C are positive, i.e., the trajectories are chaotic. We also note that the transverse Lyapunov exponents are independent of (i) the coupling function and (ii) the sizes N_1 and N_2.

The above analysis of the stability of the bipartite synchronized state compares well with the observation of two driven clusters for large ϵ values as in region IV of Fig. 1 and region III-D of Fig. 7 of Part I. We note that for both these figures the scale-free network has a tree structure which is also a bipartite network.

Now we study the periodic behavior of coupled dynamics of Eq. (25). Here we consider two cases, fixed point attractor and period two attractor.

Coupling function $g(x)=f(x)$.

Synchronization to fixed point. For the fixed point bipartite synchronized solution with one set of nodes taking the value X_1^* and the other set X_2^*, the eigenvalues for the set C or the matrix (27) are given by

$$\frac{1-\epsilon}{2}(f_1'+f_2') \pm \frac{1}{2}\sqrt{(1-\epsilon)^2(f_1'+f_2')^2 - 4(1-2\epsilon)f_1'f_2'}.$$

For the logistic map the fixed points are

$$X_{1,2}^{\star} = \frac{(1-\mu+2\mu\epsilon) \pm \sqrt{(1-\mu+2\mu\epsilon)^2 - 4\epsilon(1-\mu+2\mu\epsilon)}}{2\mu(2\epsilon-1)}. \tag{29}$$

The conditions for the stability of this solution are given by

$$|(1-\epsilon)f_{1,2}'| < 1 \tag{30}$$

and

$$\frac{1}{2}\left(1+\sqrt{\frac{3}{\mu(\mu-2)}}\right) < \epsilon < \frac{3+2\mu(\mu-2)+\sqrt{[3+2\mu(\mu-2)]^2 - 4\mu(\mu-2)(\mu-1)^2}}{4\mu(\mu-2)}. \tag{31}$$

The fixed point solution can observed in region VI-F of Fig. 7 of Part I.

Synchronization to period two orbit. The bipartite synchronous period two solution is obtained when one set of nodes takes the value X_1^p and the others take the value X_2^p and the two values alternate in time. The Jacobian matrix for the periodic orbit can be written as $J=J_1J_2$ where J_2 is obtained from J_1 [Eq. (26) with $g=f$] by interchanging f_1' and f_2'. The eigenvalues of J are given by

$$\Lambda_1 = (1-\epsilon)^2 f_1'f_2', \tag{32a}$$

$$\Lambda_{2,3} = \left(\frac{\epsilon}{2}(f') \pm \sqrt{\frac{\epsilon^2}{4}(f')^2 + (1-2\epsilon)f_1'f_2'}\right)^2, \tag{32b}$$

where Λ_1 is $(N-2)$-fold degenerate and $f'=f_1'+f_2'$. For the logistic map analytical expressions for the periodic points and the range of stability can be determined using the two conditions

$$1-\epsilon < \frac{|1-2\epsilon|}{\sqrt{(1+\mu-2\epsilon\mu)(4\epsilon-1+\mu-2\epsilon\mu)}} \tag{33}$$

and Eq. (31) with ϵ replaced by $1-\epsilon$. The values obtained using these conditions agree reasonably well with the boundaries of region II-D in Fig. 7 of Part I.

Synchronization of all nodes. The global synchronized solution where all nodes of the bipartite network are synchronized, has the Lyapunov exponents

$$\lambda_1 = \lambda_u = \lim_{\tau \text{ to } \infty} \frac{1}{\tau}\sum_{t=1}^{\tau} \ln|f'(x_t)|, \tag{34a}$$

$$\lambda_2 = \ln(1-2\epsilon) + \lambda_u, \tag{34b}$$

$$\lambda_3 = \ln(1-\epsilon) + \lambda_u, \tag{34c}$$

where λ_3 is $(N-2)$-fold degenerate. Both λ_2 and λ_3 are transverse Lyapunov exponents and the condition for stability is

$$1 - e^{-\lambda_u} < \epsilon < \frac{1}{2}(1 + e^{-\lambda_u}). \tag{35}$$

For the logistic map with $\mu=4$, this gives the range as (0.5, 0.75) and the dynamics is chaotic.

Coupling function $g(x)=x$. We will not present here the fixed point solution which is normally observed in the coherent region (V-F in Fig. 1 of Part I) and also the globally synchronized state. Here we present only the period two solution.

Synchronization to period two orbit. Consider a period two bipartite synchronized state where all nodes of one set take the value X_1 and the other set X_2 and the two values alternate in time. The Jacobian matrix $J=J_1J_2$ has an $(N-2)$-fold degenerate eigenvalue given by Eq. (32a) and the remaining two are given by

$$\Lambda_{2,3} = [\epsilon \pm (1-\epsilon)\sqrt{f_1' f_t'}]^2. \tag{36}$$

The condition for the stability of this state is

$$\max\left(1 - \frac{1}{\sqrt{f_1' f_2'}}, \frac{|f_1' f_2'| - 1}{|f_1' f_2'| + 1}\right) < \epsilon < 1. \tag{37}$$

For the logistic map periodic points can be explicitly obtained and the stability range is given by the condition

$$1 - \frac{2}{\mu^2 - 2\mu - 3} < \epsilon < 1. \tag{38}$$

Both the lower and upper bounds of ϵ match exactly with the boundaries of region IV-DP of Fig. 1 of Part I.

2. Lyapunov function analysis

For the complete bipartite networks, the Lyapunov function as defined by Eq. (15), for any two nodes belonging to the same set, is given by

$$V_{t+1}^{ij} = \{(1-\epsilon)[f(x_t^i) - f(x_t^j)]\}^2. \tag{39}$$

Expanding around x_t^j gives the ratio of Lyapunov functions at two successive times,

$$\frac{V_{t+1}^{ij}}{V_t^{ij}} = (1-\epsilon)^2\left[f'(x_t^j) + \frac{x_t^i - x_t^j}{2} f''(x_t^j) + O((x_t^i - x_t^j)^2)\right]^2. \tag{40}$$

If the term in the square bracket on the right-hand side is bounded then there will be a critical value of ϵ beyond which $V_{t+1}^{ij}/V_t^{ij} < 1$ and thus the bipartite synchronized state will be stable.

We see that for driven synchronization, the Lyapunov function for any pair of nodes belonging to the same set does not depend on the size of the complete bipartite network and the type of coupling because in the expression for the Lyapunov function, the contribution of such couplings cancel out. This is not the case for the globally coupled networks where contribution of the coupling terms for the two nodes under consideration do not exactly cancel [Eq. (18)] and the size of the network has an effect on the dynamical behavior.

For the logistic map and using $0 \leqslant x_t^i + x_t^j \leqslant 2$ and Eq. (17), we get the following range of ϵ values for synchronization of nodes i and j,

$$\frac{\mu - 1}{\mu} \leqslant \epsilon \leqslant 1. \tag{41}$$

A better ϵ range can be obtained by taking a more appropriate boundary as $X^- < x_t^i + x_t^j < X^+$, which gives

$$1 - \frac{1}{\mu A} < \epsilon \leqslant 1, \tag{42}$$

where A is defined after Eq. (21).

C. Self-organized and driven synchronization

The analysis presented so far sheds some light on the dynamical origin of the two types of synchronization, namely self-organized and driven, that we have studied. In self-organized synchronization the clusters have dominant intracluster couplings while in driven synchronization the clusters have dominant intercluster couplings. We consider globally coupled networks as simple examples of self-organized synchronization while complete bipartite networks as simple examples of driven synchronization.

From the expression (18) for the Lyapunov function we see that in the dynamics of the globally coupled networks the direct coupling term between the two nodes under consideration appears in the expression for the Lyapunov function while the coupling terms to other variables cancel out. On the other hand, from Eq. (39) we see that in the expression for the Lyapunov function for two nodes for the complete bipartite network the coupling terms with the other variables cancel out.

The stability analysis presented here is for exact synchronization while numerical work presented in Part I considers phase synchronized clusters. However, we feel that the dynamical origin for the two mechanisms of cluster formation should be similar in both cases. Also the stability analysis is carried out for some simple networks while the numerical work is carried out on various realistic networks. We have compared several features such as phase space plots, largest Lyapunov exponent, f_{inter} and f_{intra} for the complete bipartite networks and the corresponding plots for several networks considered in the numerical work and we find considerable similarity in the features. As an example we show in Figs. 1(a) and 1(b) f_{inter} and f_{intra} as a function of ϵ, respectively, for $g(x)=x$ and $g(x)=f(x)$ and for $\mu=4$ and a complete bipartite network of 50 nodes with $N_1=N_2=25$. The similar features of these figures and the corresponding figures for the scale-free networks (Figs. 4 and 9 of Part I) are obvious. The similarity between the findings of the stability analysis and the features of the numerical phase space plots is also pointed out in several places in the previous sections. Thus the stability analysis of the synchronized cluster on simple analytically tractable networks can be useful in understanding the behavior of more complex networks.

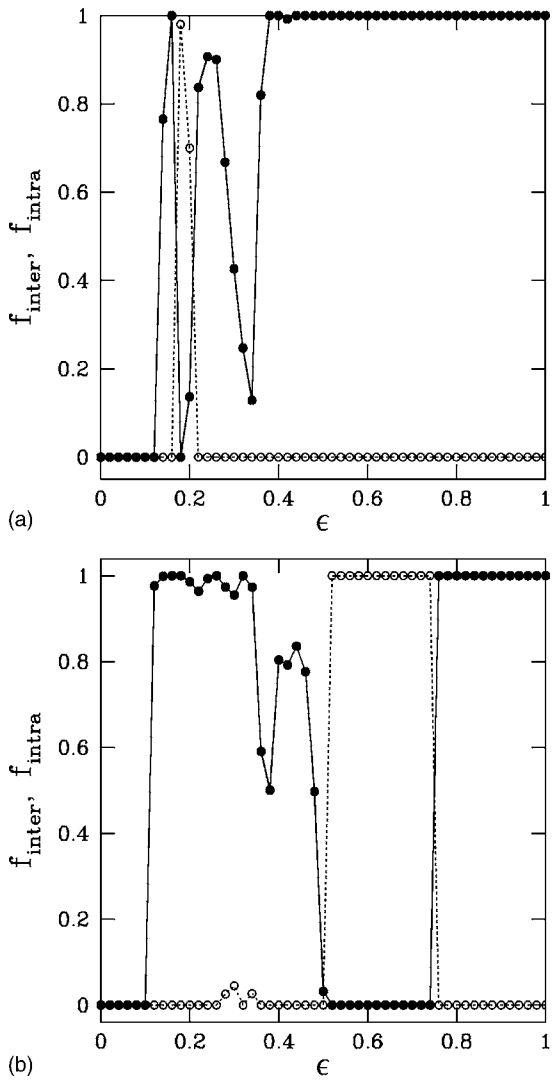

FIG. 1. (a) The figure shows the fractions of inter- and intracluster couplings, f_{inter} (closed circles) and f_{intra}, (open circles), as a function of the coupling strength ϵ for a complete bipartite network with $N_1=N_2=25$, logistic map as local map with $\mu=4$ and $g(x)=x$. The lines connect the points and are drawn as a guide to the eye. The values are obtained by averaging over 50 random initial conditions. (b) Same as for (a) but for $g(x)=f(x)$.

D. Complete multipartite networks

The stability analysis for the complete bipartite networks can be easily extended to complete multipartite networks. Consider a complete M-partite network of M parts, consisting of $N_i, i=1,\ldots,M$ nodes each. There are no intrapart connections. Nodes of any pair of parts are either not connected or completely connected to each other. The M-partite synchronized state corresponds to nodes of each part being synchronized to some value, say X_i. As in the bipartite case the eigenvalues and eigenvectors can be divided into $M+1$ orthogonal sets with N_i-1, $i=1,\ldots,M$, and M elements, respectively. The last set of M elements defines the synchronization manifold while the others are transverse manifolds. There are M distinct transverse eigenvalues $(1-\epsilon)f'(X_i)$ with degeneracies N_i-1. The condition for the stability of the synchronized state is that all the corresponding transverse Lyapunov exponents are negative. Clearly the analysis of the corresponding range of stability of the M-partite synchronized state will be very similar to that of the complete bipartite networks.

E. Comparison between analytical and numerical results

In this section we have presented stability analysis of the synchronized states for some simple networks, a globally connected network, and a complete bipartite network. In several places we have pointed out the similarity of these results with those observed numerically for more complex networks in Part I. The similarity is striking in several places and thus the stability analysis of these simple networks helps us in the understanding of the synchronization structure of more complex networks. Here we discuss the possible reasons for this similarity.

Pecora and Carroll [17] have shown that the linear stability analysis of the complete synchronized state of complex networks can be done using a master stability function. The analysis of the master stability function can be done without reference to any particular network and the range of stability of the complete synchronized state can be determined. For any given network, stability of the complete synchronized state can be decided as follows. The eigenvalues of the adjacency (or Laplacian) matrix for the network can be arranged as $0=\lambda_1 \geqslant \lambda_2 \geqslant \ldots \geqslant \lambda_N$. The eigenvalue λ_1 corresponds to the synchronization manifold. The remaining eigenvalues must satisfy the condition $\epsilon\lambda_i \in (\alpha_1, \alpha_2)$ where α_1 and α_2 are determined using the master stability function. Thus the details of the network are not important and only the spectrum of eigenvalues determines the linear stability of the complete synchronized state. Hence networks which have a similar eigenvalue spectrum or more precisely nearly the same eigenvalues corresponding to the largest transverse Lyapunov exponent will have a similar stability property of the complete synchronized state. Thus networks which have similar structures are expected to have similar stability properties of the synchronized state and the details of the network are not important.

The above analysis is for the complete synchronized state. A similar stability analysis for the multicluster state in terms of master stability function can be carried out [18]. Hence we expect similar reasoning to hold for the multicluster state as well and hence structurally similar networks should have similar stability properties.

III. FLOATING NODES

As discussed in Part I, the nodes of a network can be divided into three types based on their asymptotic dynamical behavior, namely (a) cluster nodes: These nodes remain in a synchronized cluster for all the time, (b) isolated nodes: these nodes do not belong to a synchronized cluster at any time, and (c) floating nodes: these nodes show an intermittent behavior between evolution synchronized with some cluster and isolated evolution. Here we try to analyze the reasons for the occurrence of the floating nodes.

Consider a floating node in a cluster. The stability of this cluster is ensured if the transverse Lyapunov exponents are all negative. The floating node will leave the cluster provided the conditional Lyapunov exponent for this node, assuming that the other nodes in the cluster remain synchronized, must change sign, and become positive. Thus the fluctuation of the conditional Lyapunov exponent about zero can be taken as the condition for the existence of a floating node [19].

Consider a floating node of degree k such that there are k_1 connections to nodes belonging to the cluster with which it intermittently synchronizes and $k_2=k-k_1$ connections to nodes outside the cluster. Consider an evolution when the floating node is synchronized with the cluster. The dynamics of the floating node is given by

$$x_{t+1} = (1-\epsilon) f(x_t) + \frac{\epsilon}{k}\left(k_1 g(x_t) + \sum_{i=1}^{k_2} g(x_t^j) \right). \tag{43}$$

Assume that the other nodes of the cluster remain in the synchronized state. Hence small deviation δx_t of the floating node evolves as

$$\delta x_{t+1} = (1-\epsilon) f'(x_t)\delta x_t + \frac{\epsilon}{k}\sum_{i=1}^{k_2} g'(x_t^i)\delta x_t^i. \tag{44}$$

Since the other nodes in the cluster remain in the synchronized state, we expect that on the average $|(1-\epsilon)f'(x_t)|<1$ [see the expressions for the transverse Lyapunov exponents in Eq. (5b) for large N and Eq. (28)]. Hence the floating node can leave the cluster only if the magnitude of the second term in Eq. (44) is sufficiently large to overcome the first term. For this to happen, one or more of the following possibilities exist:

(1) k_2 is large;

(2) these k_2 nodes do not belong to a single synchronized cluster; and

(3) the k_2 nodes evolve chaotically.

The numerical observation of the floating nodes supports these observations. We note that the floating nodes are observed in the partially ordered region (region III in Figs. 1 and 7 of Part I) where the evolution is chaotic. There are several clusters and isolated nodes and the floating nodes in general have some connections to other isolated or floating nodes.

Though the above analysis is still not sufficient for identifying the exact nodes which show floating behavior, it does give us some understanding of why and when a node can be a floating node.

IV. CONCLUSION

We have studied the stability of self-organized and driven synchronization in two simple coupled map networks, namely globally coupled and complete bipartite networks using both linear stability analysis and the Lyapunov function approach. For the globally coupled network we analyze the globally synchronized state while for the complete bipartite network we analyze the bipartite synchronized state. We also consider fixed point and period two synchronized states. The linear stability analysis gives different regions of phase space where different states are stable. The interesting observation of the study is that the phase diagrams for the simple networks studied here, particularly the complete bipartite networks, have features very similar to the different kinds of networks studied in Part I. This is more striking if we note that in Part I we have used phase synchronization while for the stability analysis we use perfect synchronization. Thus analytic studies of simple networks can be useful in understanding the synchronization properties of more complex networks.

From the Lyapunov function approach we see that for the difference of the dynamical variables for any two nodes that are in driven synchronization, all the coupling terms cancel out. On the other hand, when they are in self-organized synchronization the coupling terms corresponding to the direct coupling between the two nodes under consideration do not cancel out, though coupling terms for couplings to other nodes may cancel.

We have also made a simple analysis of the dynamics of a floating node. We suggest that the fluctuation of the conditional Lyapunov exponent about zero, assuming that the other nodes belonging to the synchronized cluster remain synchronized, can be a criterion for the existence of a fluctuating node. Conclusions drawn using this criterion are consistent with the numerical observations.

ACKNOWLEDGMENTS

This work was partly supported by National Science Council of Taiwan under Grant No. NSC 92-2112-M 001-063 and Academia Sinica under Grant No. AS-91-TP-A02. One of us (R.E.A.) will like to thank Physics Division of National Center for Theoretical Sciences at Taipei and Institute of Physics of Academia Sinica for hospitality where the final version of this paper was done.

[1] S. Jalan, R. E. Amritkar, and C.-K. Hu, Phys. Rev. E **72**, 016211 (2005) and references therein.

[2] S. Jalan and R. E. Amritkar, Phys. Rev. Lett. **90**, 014101 (2003); R. E. Amritkar and S. Jalan, Physica A **321**, 220 (2003).

[3] H. Fujisaka and T. Yamada, Philos. Trans. R. Soc. London **69**, 32 (1983); **74**, 918 (1985).

[4] P. M. Gade, Phys. Rev. E **54**, 64 (1996).

[5] M. Ding and W. Yang, Phys. Rev. E **56**, 4009 (1997).

[6] R. E. Amritkar, P. M. Gade, A. D. Gangal, and V. M. Nandkumaran, Phys. Rev. A **44**, R3407 (1991).

[7] Q. Zhilin and G. Hu, Phys. Rev. E **49**, 1099 (1994).

[8] M. Soins and S. Zhou, Physica D **165**, 12 (2002).
[9] Y. Chen, G. Rangarajan, and M. Ding, Phys. Rev. E **67**, 026209 (2003).
[10] S. Wiggins, *Introduction to Applied Nonlinear Dynamical Systems and Chaos* (Springer-Verlag, Berlin, 1990).
[11] R. He and P. G. Vaidya, Phys. Rev. A **46**, 7387 (1992); Phys. Rev. E **57**, 1532 (1998).
[12] K. Kaneko, Phys. Rev. Lett. **65**, 1391 (1990); **41**, 137 (1990); **124**, 322 (1998).
[13] Y. L. Maistrenko, V. L. Maistrenko, O. Popovych, and E. Mosekilde, Phys. Rev. E **60**, 2817 (1999).
[14] Y. Kuramoto, *Chemical Oscillations, Waves, and Turbulence* (Springer-Verlag, Berlin, 1984).
[15] A. Pikovsky, M. Rosenblum, and J. Kurth, *Synchronization: A Universal Concept in Nonlinear Dynamics* (Cambridge University Press, Cambridge, England, 2001).
[16] In this case the increased range of stability with increasing N is accompanied by a decrease in the basin of attraction. Hence numerically starting from random initial conditions this incremental part of the range is not easily observed.
[17] L. M. Pecora and T. L. Carroll, Phys. Rev. Lett. **80**, 2109 (1998).
[18] R. E. Amritkar (unpublished).
[19] Flutuation of a Lyapunov exponent about zero indicates that the shadowing lemma may not be valid [20]. But, the conditional Lyapunov exponent which we use here is in general different from the unconditional Lyapunov exponent. It is not clear whether a similar criterion for the validity of the shadowing lemma also exists for a conditional Lyapunov exponent.
[20] S. Dawson, C. Grebogi, T. Sauer, and J. A. Yorke, Phys. Rev. Lett. **73**, 1927 (1994).